U.S. DEPARTMENT OF THE INTERIOR
U.S. GEOLOGICAL SURVEY

EXPERIMENTAL TESTING OF FLEXIBLE BARRIERS FOR CONTAINMENT OF DEBRIS FLOWS

by

Jay S. DeNatale[1]
Richard M. Iverson[2]
Jon J. Major[2]
Richard G. LaHusen[2]
Gregg L. Fiegel[1]
John D. Duffy[1]

[1] *California Polytechnic State University*
Civil and Environmental Engineering Department
1 Grand Avenue
San Luis Obispo, California 93407

[2] *United States Geological Survey*
David A. Johnston Cascades Volcano Observatory
5400 MacArthur Boulevard
Vancouver, Washington 98661

OPEN-FILE REPORT 99-205

Vanvcouver, Washington
1999

U.S. DEPARTMENT OF THE INTERIOR

BRUCE BABBIT, *Secretary*

U.S. GEOLOGICAL SURVEY

Charles G. Groat, *Director*

For additional information
write to:

U.S. Geological Survey
Cascades Volcano Observatory
5400 MacArthur Boulevard
Vancouver, Washington 98661

Copies of this report
can be purchased from:

U.S. Geological Survey
Branch of Distribution
Federal Center, Box 25286
Denver, CO 80225

CONTENTS

ILLUSTRATIONS

Figure Page

TABLES

Table Page

CONVERSION FACTORS

Multiply	by	To obtain
	Length	
millimeter (mm)	0.03937	inch
centimeter (cm)	0.3937	inch
meter (m)	3.281	foot
	Area	
square meter (m^2)	10.76	square foot
	1.196	square yard
	Volume	
cubic meter (m^3)	35.31	cubic feet
	1.308	cubic yard
	Speed	
meter per second (m/s)	3.281	foot per second
	2.237	mile per hour
	Mass	
kilogram (kg)	0.06854	slug
	2.205	pound (mass)
metric ton (Mg)	1.102	ton (mass)
	Force	
Newton (N)	0.2248	pound (force)
kiloNewton (kN)	0.1124	ton (force)

ABSTRACT

In June 1996, six experiments conducted at the U.S. Geological Survey Debris Flow Flume demonstrated that flexible, vertical barriers constructed of wire rope netting can stop small debris flows. All experimental debris flows consisted of water-saturated gravelly sand with less than two percent finer sediment by weight. All debris flows had volumes of about 10 cubic meters, masses of about 20 metric tons, and impact velocities of 5 to 9 meters per second. In four experiments, the debris flow impacted pristine, undeformed barriers of varying design; in the other two experiments, the debris flow impacted barriers already loaded with sediment from a previous flow.

Differences in barrier design led to differences in barrier performance. Experiments were conducted with barriers constructed of square-mesh wire-rope netting with 30 centimeter, 20 centimeter, and 15 centimeter mesh openings as well as 30 centimeter diameter interlocking steel rings. In all cases, sediment cascading downslope at the leading edge of the debris flows tended to spray through the nets. Nets fitted with finer-mesh chain link or chicken wire liners contained more sediment than did unlined nets, and a ring net fitted with a synthetic silt screen liner contained nearly 100 percent of the sediment. Irreversible net displacements of up to 2 meters and friction brake engagement on the support and anchor cables dissipated some of the impact energy. However, substantial forces developed in the steel support columns and the lateral and tie-back anchor cables attached to these columns. As predicted by elementary mechanics, the anchor cables experienced larger tensile forces when the support columns were

hinged at the base rather than bolted rigidly to the foundation. Measured loads in the lateral anchor cables exceeded those in the tie-back anchor cables and the load cell capacity of 45 kilo-Newtons. Measurements also indicated that the peak loads in the tie-back anchors were highly transient and occurred at the points of maximum momentum impulse to the net.

INTRODUCTION

During the winter of 1994-95, a flexible wire rope rock net installed along California State Route 41 in San Luis Obispo County stopped and contained several rainfall-induced debris flows having a combined volume of approximately 60 m^3 (cubic meters) (Duffy and DeNatale, 1996). In June 1996, a limited experimental study was undertaken to establish, in a more quantitative fashion, the response of such flexible systems to debris-flow loading.

Experiments were performed at the United States Geological Survey (USGS) Debris Flow Flume located within the H. J. Andrews Experimental Forest near Blue River, Oregon. The flume is a reinforced concrete channel 95 m (meters) long, 2 m wide, and 1.2 m deep. The uppermost 88 m of the flume bed lie at an angle of 31 degrees and the lowermost 7 m gradually flatten to a run-out slope of 3 degrees. A concrete run-out pad at this same 3 degree slope extends 25 m beyond the mouth of the flume. Up to 20 m^3 of water-saturated sediment can be discharged from the mouth of the flume at velocities of approximately 10 m/s (meters per second) (Iverson and others, 1992). The "debris" employed during the June 1996 experiments consisted of a poorly graded, clean, gravelly sand that had been used in previous USGS debris flow studies (Iverson, 1997; Major and others, 1997).

Massive 1.22 m wide concrete panels can be placed on the concrete run-out pad to confine the flow beyond the mouth of the flume. In the June 1996 experiments, eight confinement panels were placed to provide an additional 5 m of channelized flow. This

arrangement ensured that the flow would not spread laterally prior to its impact with the flexible barrier. A schematic plan view of the experiment configuration is shown in figure 1.

In the June 1996 experiments, a load cell and two piezometers were placed in a port within the run-out pad (1 m behind the flexible barrier) to record the vertical total stress and pore fluid stress that developed at the base of the deposit. An ultrasonic flow depth sensor was attached to a support beam that crossed this same section. An extensometer was attached to the front of the net to record the history of net deformation in the direction of flow. Load cells were installed in two of the four barrier anchor cables to measure the history of tensile force sustained by these key structural components. A high-frequency digital data acquisition system permitted continuous, synchronous recording of all instrument signals. The kinematics of the flow and barrier response were documented through still and video camera surveillance during each flow. A topographic survey of the deposit was done at the conclusion of each flow.

This report summarizes basic experimental data that bear on the performance of the flexible barrier systems. The data lead to the conclusion that some such systems can effectively contain debris flows with volumes of about 10 m^3 and speeds less than 10 m/s.

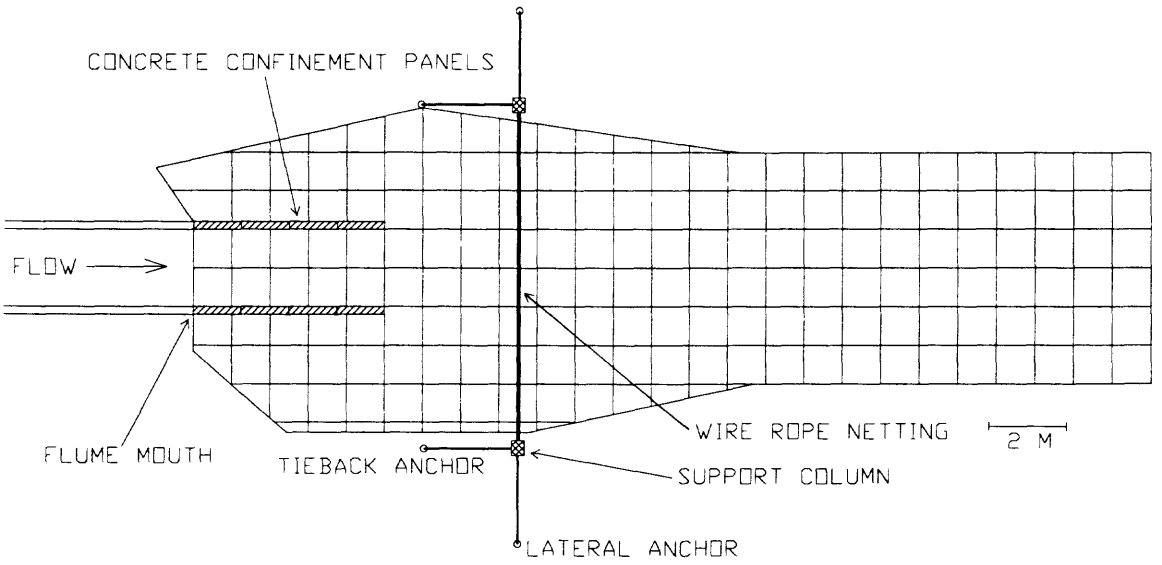

Figure 1. Schematic plan view of the barrier placement on the run-out pad.

BARRIER CONFIGURATION

Six tests were conducted with four different flexible barriers. All barriers had a height of 2.4 m and a length of 9.1 m, sufficient to completely span the flume's concrete run out pad, as shown in figure 1.

The first barrier system (test 1) employed 30 cm by 30 cm wire rope netting overlaid with a 5.1 cm chain link liner to reduce the size of the largest clear opening. The net panel was supported by 1.9 cm diameter perimeter and anchor cables and two vertical W 4 x 13 structural steel columns rigidly fixed to concrete anchor pads. W 4 x 13 is the American Institute for Steel Construction (AISC) designation for a wide-flange section having a nominal depth of 4 inches and a weight of 13 pounds/lineal foot. Photographs taken before and after the debris flow are included as figures 2 and 3.

The second barrier system (tests 2 and 3) employed 20 cm by 20 cm wire rope netting overlaid with a 5 cm chain link liner. An additional chicken wire liner was attached to the middle third of the net to further reduce the size of the largest clear opening. The net panel was supported by 1.9 cm diameter perimeter and anchor cables and hinged-base steel columns. The barrier was subjected to two consecutive debris flows. Photographs taken during and after the debris flow are included as figures 4-7.

The third barrier system (tests 4 and 5) employed 15 cm by 15 cm wire rope netting overlaid with full-width chain link and chicken wire liners. The net panel was supported by 1.9 cm diameter perimeter and anchor cables and W 8 x 48 fixed-base steel

columns. The barrier was subjected to two consecutive debris flows. Photographs taken before, during and after the debris flow are included as figures 8-11.

The fourth barrier system (test 6) employed 30 cm diameter interlocking rings overlaid with full-width chain link and silt screen liners. The net panel was supported by 1.9 cm diameter perimeter and anchor cables and W 8 x 48 fixed-base steel columns. Photographs taken before and after the debris flow are included as figures 12 and 13.

The rope nets used in tests 1-5 were fabricated using galvanized wire rope with a diameter of 0.8 cm and a nominal breaking strength of 40.9 kN. Each "ring" of the ring net used in test 6 consisted of a bundle of four steel rings, each with a cross-sectional diameter of 0.3 cm.

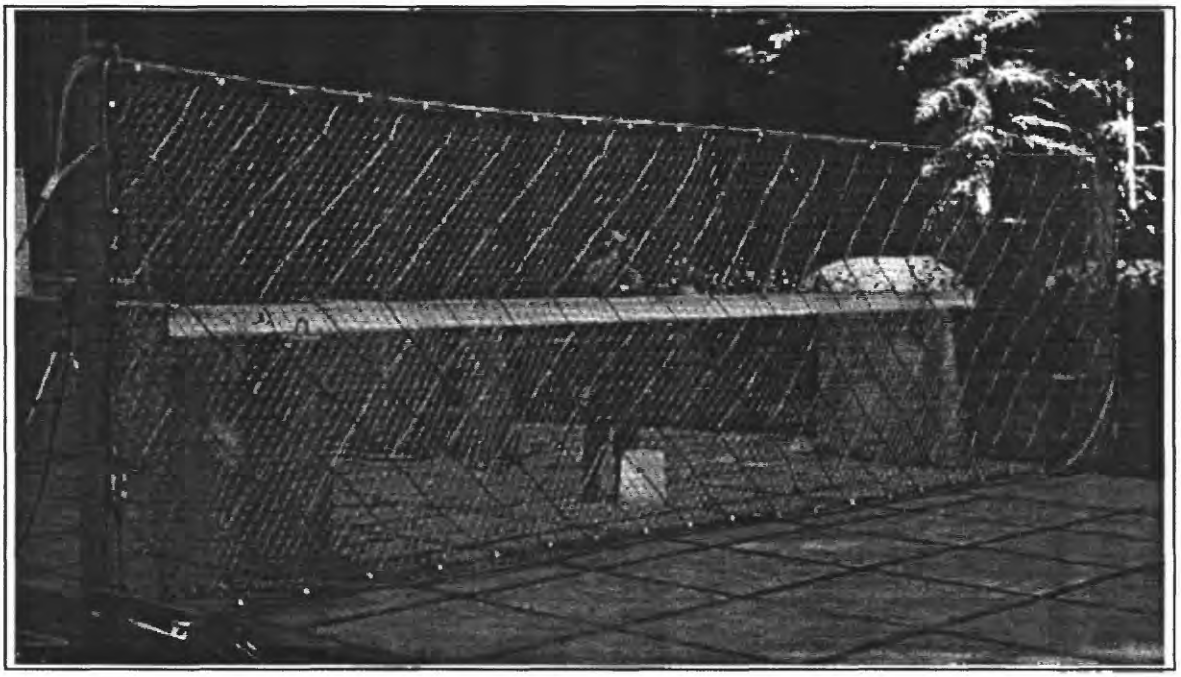

Figure 2. Barrier 1 (test 1).

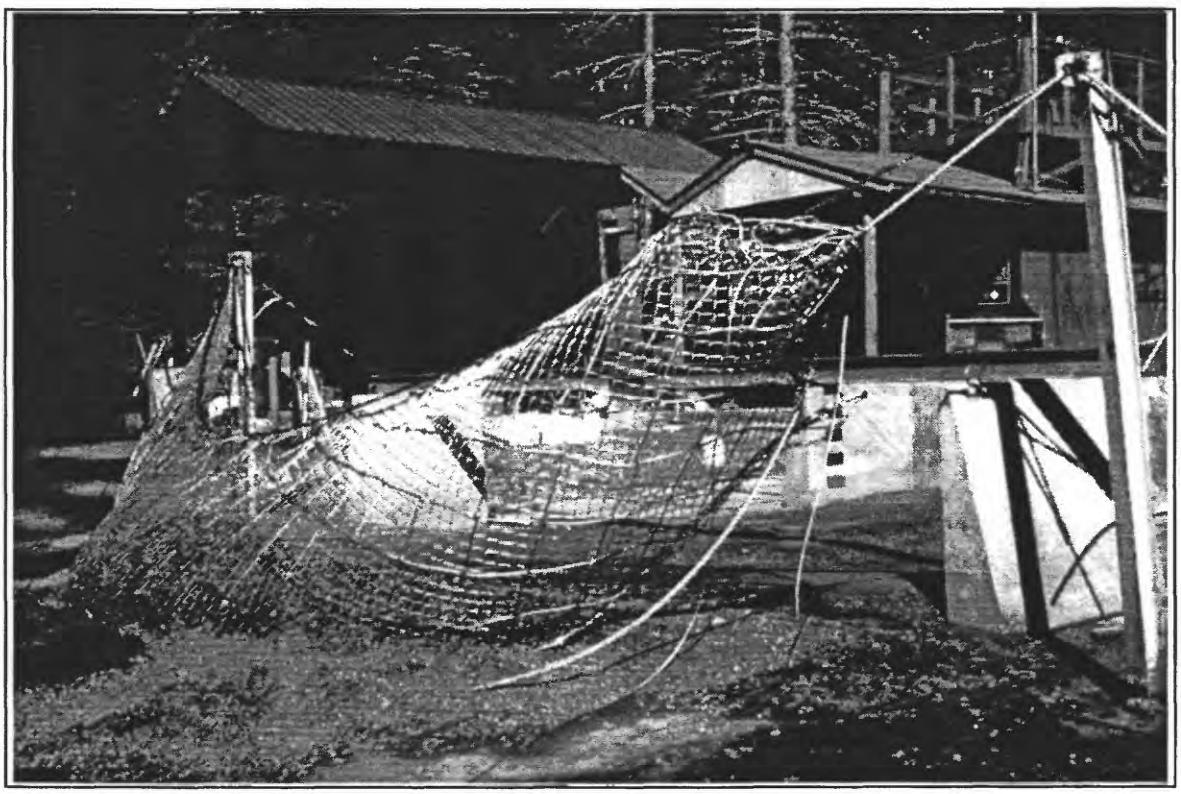

Figure 3. Post-flow condition of barrier 1 (test 1).

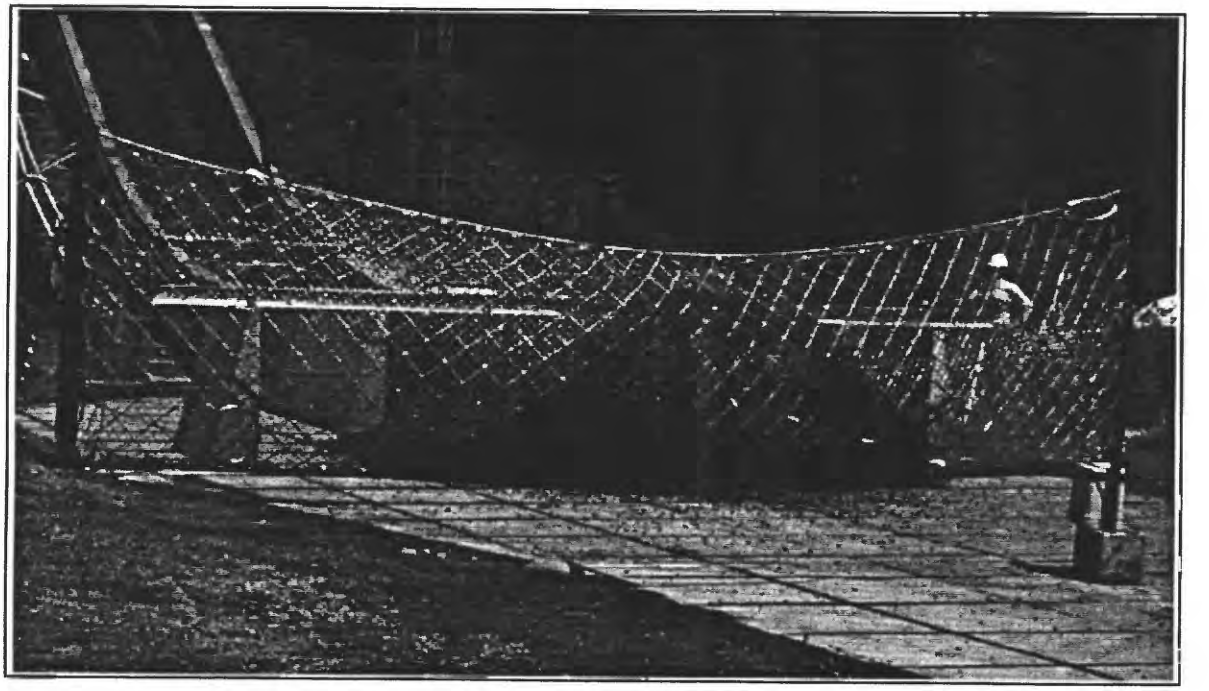

Figure 4. Maximum run-up on barrier 2 (test 2).

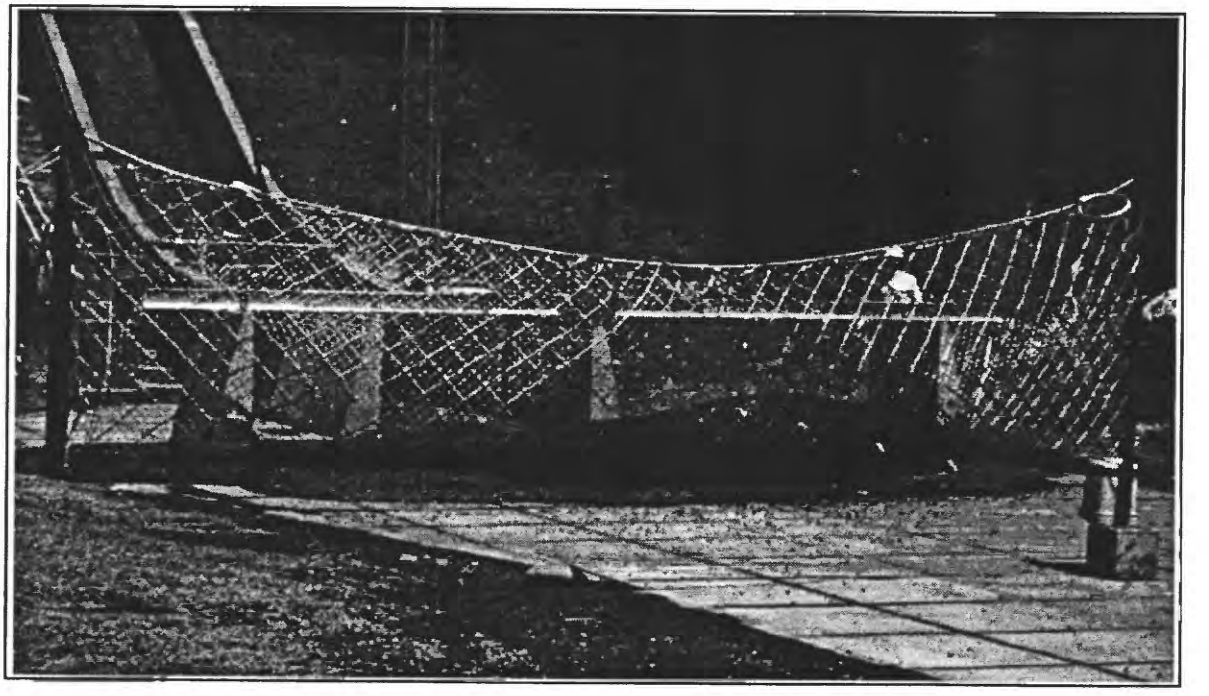

Figure 5. Post-flow condition of barrier 2 (test 2).

Figure 6. Collapse of right column and overtopping of barrier 2 (test 3).

Figure 7. Post-flow profile view of barrier 2 (test 3).

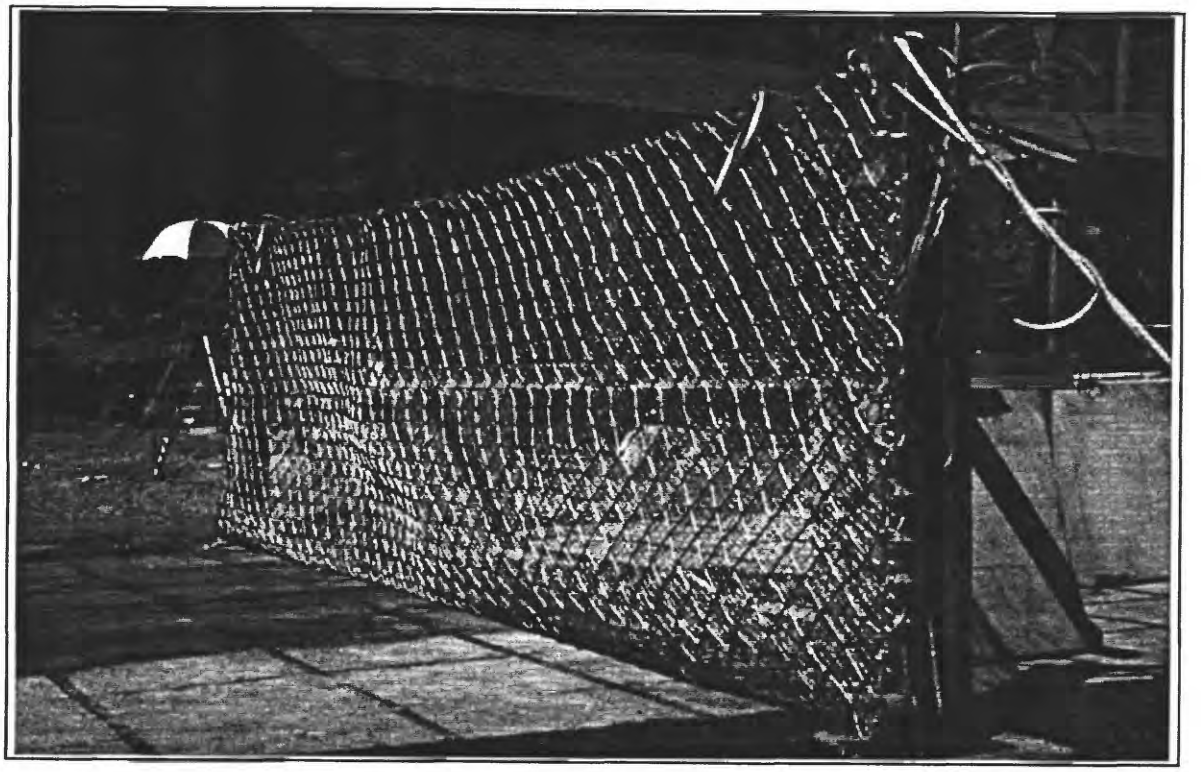

Figure 8. Barrier 3 (test 4).

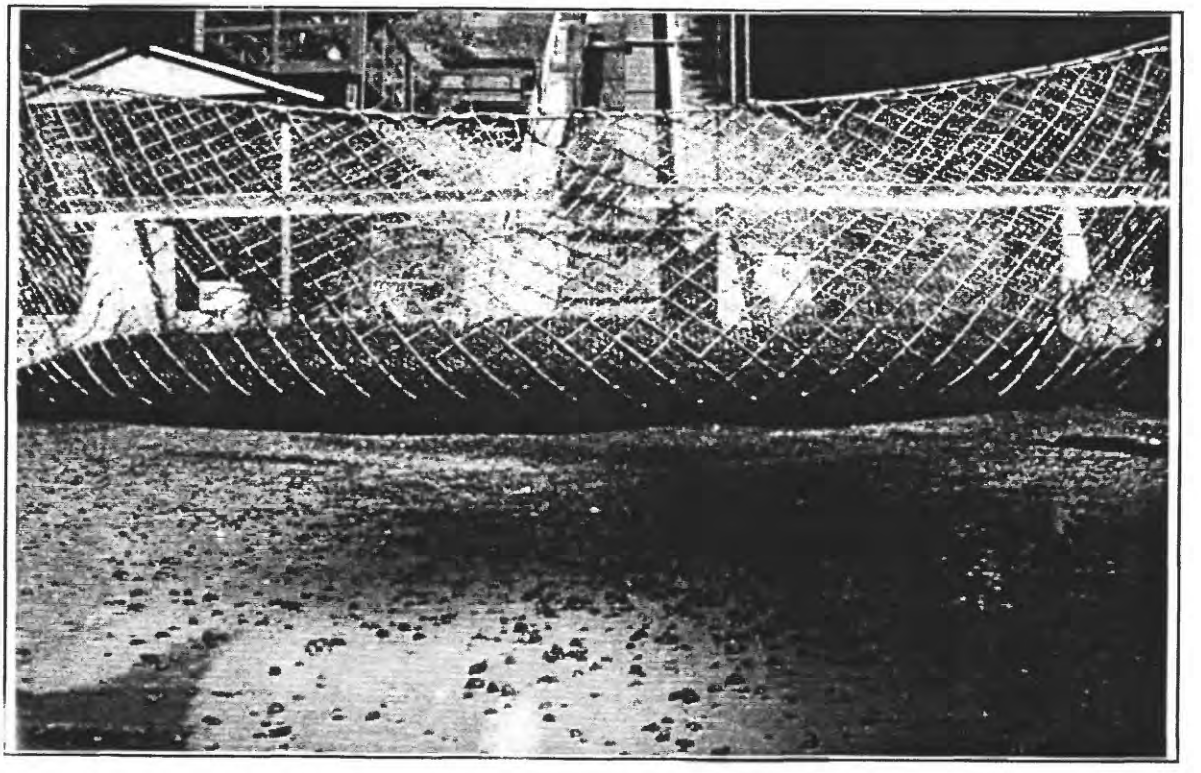

Figure 9. Post-flow frontal view of barrier 3 (test 4).

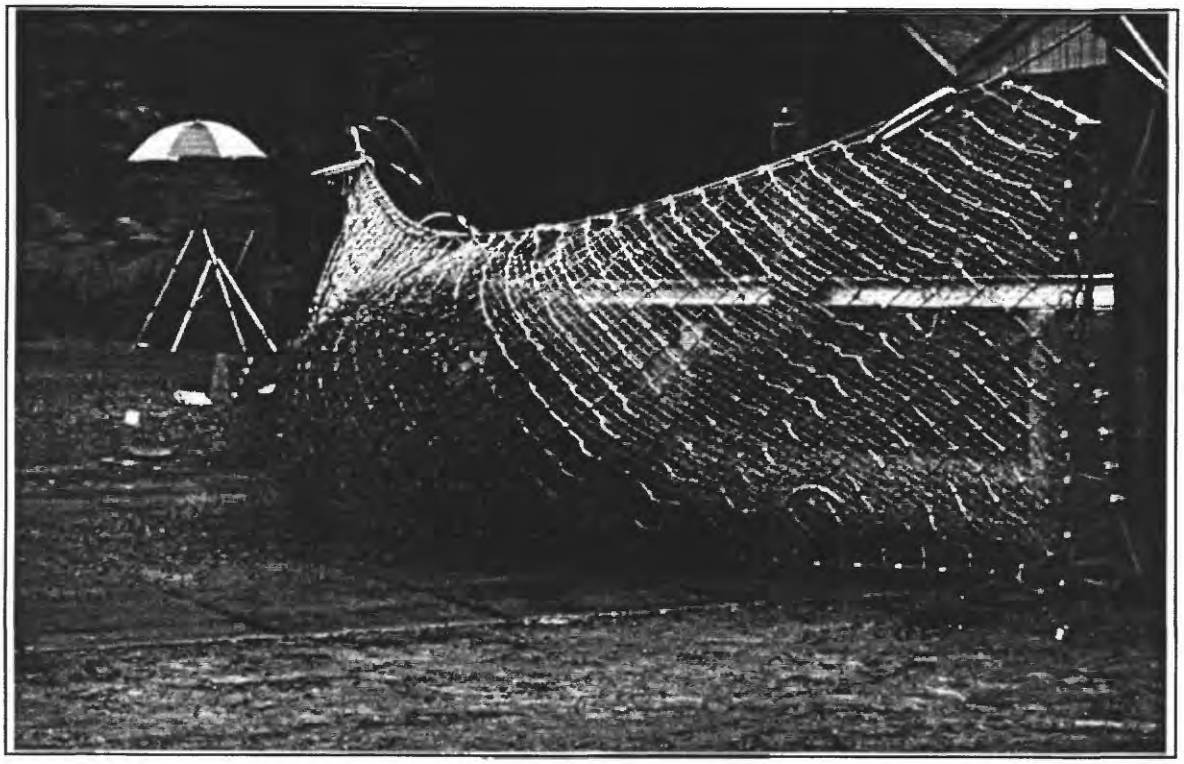

Figure 10. Maximum run-up on barrier 3 (test 5).

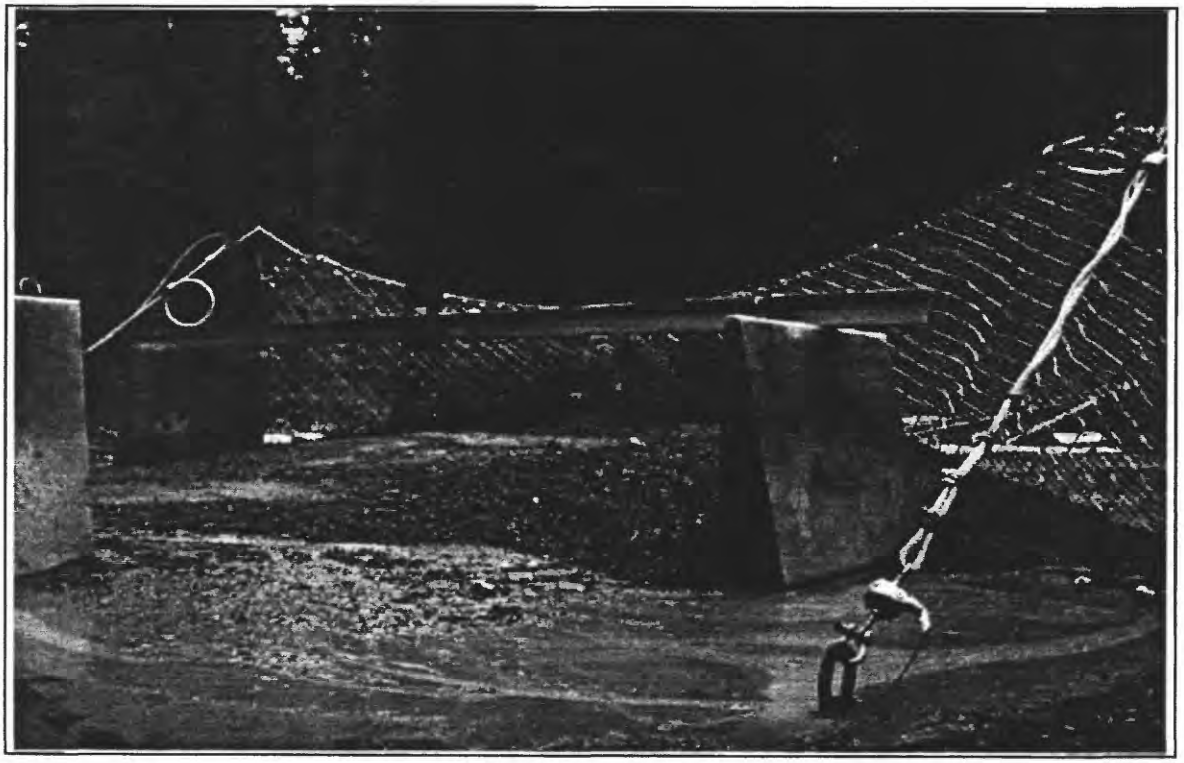

Figure 11. Debris deposition behind barrier 3 (test 5).

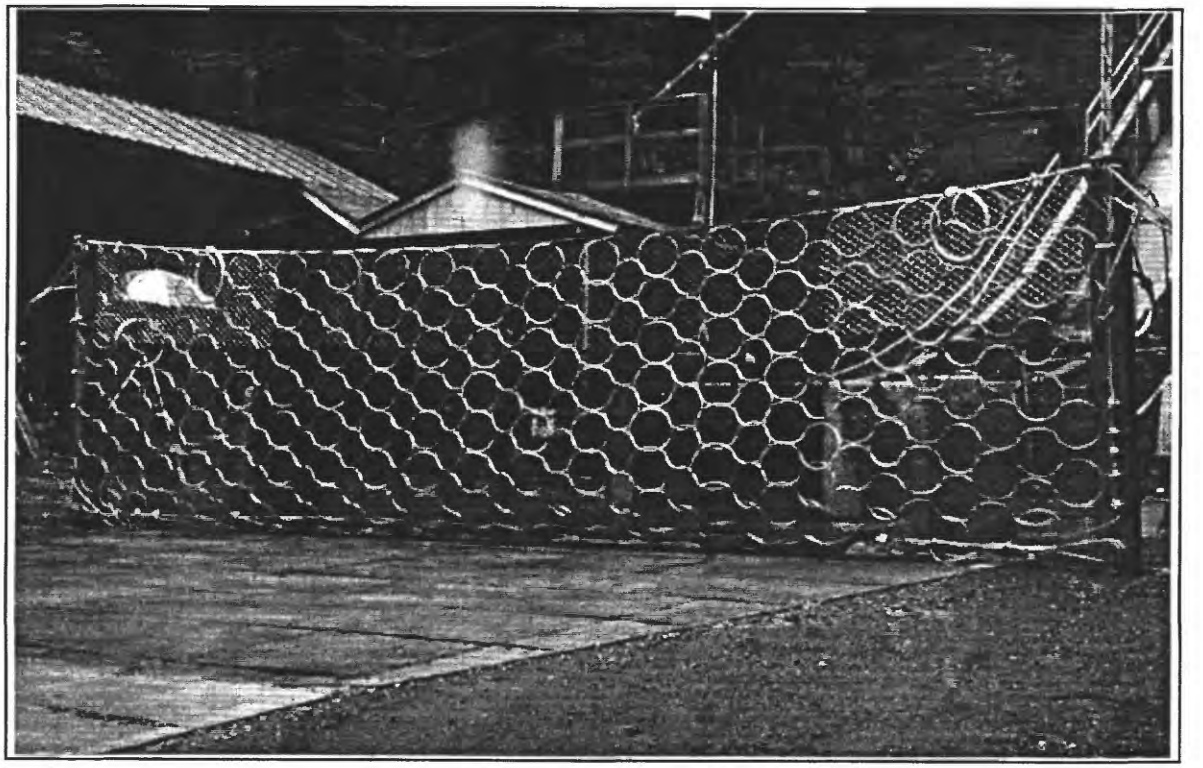

Figure 12. Barrier 4 (test 6).

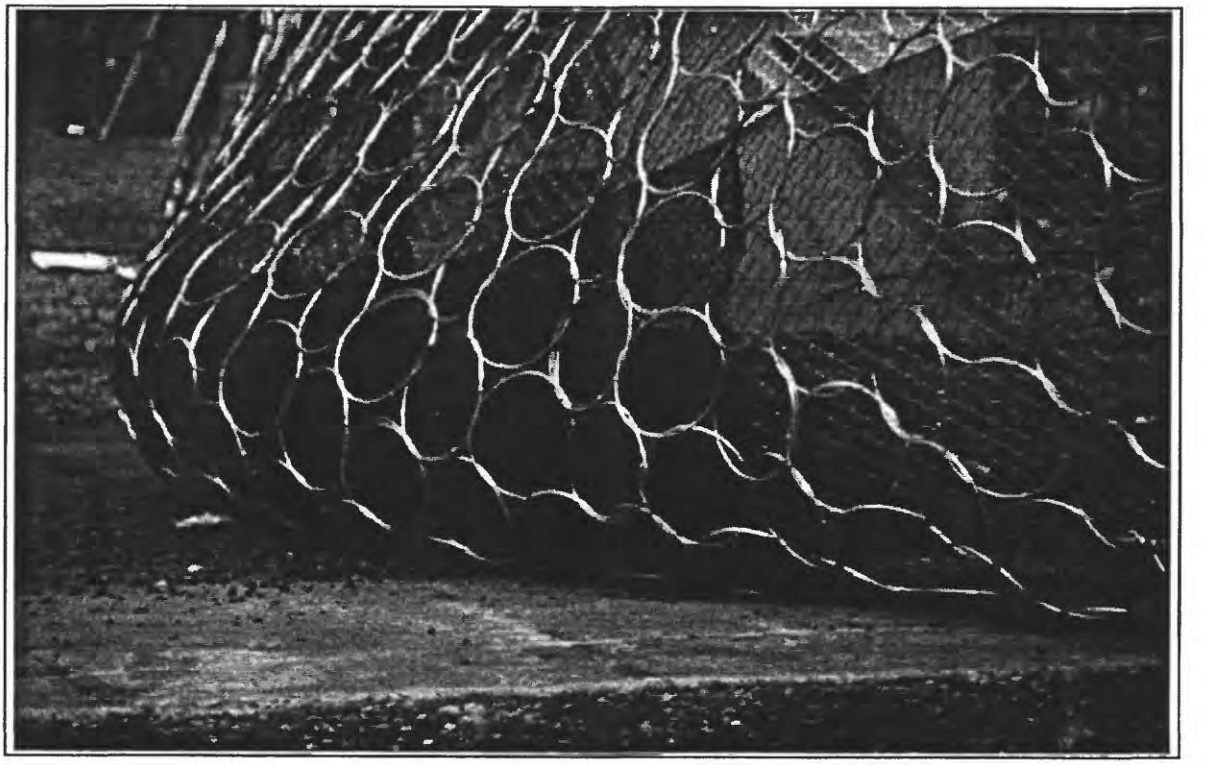

Figure 13. Post-flow condition of barrier 4 (test 6).

BARRIER PERFORMANCE

Debris volume, flow velocity, and barrier deflection data measured during the six experiments are compared in table 1. Flow velocities were derived from the time-stamped videotape records acquired with an overhead camera. The concrete run-out pad is marked with a set of one meter square gridlines. Velocities were obtained by noting the time required for certain readily identifiable debris (such as the gravel spray, chunks of foam sealant, and/or wave fronts) to pass from one grid line to another.

Barrier deflection in the direction of flow was recorded by a cable extensometer that was attached to the net at mid-span, at a point 50 cm above the run-out pad. Deflection data are compared in figure 14. The three successful barrier systems experienced comparable degrees of outward deflection during the first loading cycle (tests 2, 4, and 6). In all three cases, the maximum deflection was between 1.5 and 2.0 m. A second release of debris into an already loaded net (tests 3 and 5) produced less than one-half meter of additional outward movement.

One objective of the June 1996 field testing program was to establish the degree to which relatively open and porous flexible barriers could stop and contain rapidly moving, staged debris flows. Hence, measurements were made of the volume and spatial distribution of the material that passed beneath or through each net.

A comparison of barrier effectiveness in terms of debris containment is presented in table 2. The first two barrier systems incorporated chain link net panel liners to reduce the size of the largest net opening. The first barrier system (test 1) experienced a support

column failure and collapsed during the flow. The second barrier system performed well during the initial debris flow (test 2) but experienced an anchor cable connection failure and partially collapsed during the subsequent debris flow (test 3). The last two barrier systems incorporated both chain link and chicken wire (tests 4 and 5) or silt screen (test 6) net panel liners. As shown in table 2, each barrier stopped and contained most of the flowing debris. Essentially full containment was realized in test 6, where less than 0.05 percent of the sediment passed beneath or through the net.

Laboratory sieve analyses were done to determine the gradation characteristics of sediment samples recovered at the conclusion of each debris flow. The dry mass of these samples ranged from 2.6 to 17.0 kg (kilograms). Grain size distribution curves of the passed and retained materials are compared in figures 15-18. In tests 4 and 6, the passed material consisted almost entirely of gravel-sized particles (fig. 16 and 17). As expected, somewhat more sand passed through the chicken wire than the finer-mesh silt screen (fig. 18). Photographs reveal that a very diffuse spray of gravel always precedes the first wave of flowing debris. It is this diffuse spray (and only this spray) that passed beneath and through the net. Most of the passed material came to rest very quickly. In test 6, for example, only 12.5 percent of the passed material (0.006 percent of the initial volume) flowed more than 3 m beyond the net (fig. 19).

In general, there was little or no lateral flow around the left and right edges of the barrier. Contours of the standing debris deposits derived from the post-flow topographic survey data are shown in figures 20-25.

Tensile forces in the lateral and tie-back (upslope) anchor cables were measured by installing 45 kN load cells between the anchor cables and the ground anchors (rock bolts). The anchor cable forces measured during tests 1-6 are shown in figures 26-31, respectively. In the first three experiments, one cell was installed in the right lateral anchor cable and one cell was installed in the right tie-back anchor cable.

In test 1 (fig. 26), the signal gain was set too high and cable forces in excess of 10 kN could not be logged. The gain was set lower in all subsequent tests. In test 2 (fig. 27), the lateral anchor force peaked at 40 kN (90 percent of the cell's capacity). In test 3 (fig. 27), the lateral anchor force reached 42 kN (95 percent of the cell's capacity) before the threaded bolt pulled out from the cell base. Although frustrating, this connection failure may have been serendipitous, for it prevented the cell from being overloaded and permanently damaged. Prior to test 4, the cell was removed from the right lateral anchor cable and placed in the left tie-back anchor cable.

Elementary mechanics reveals that the anchor force in a cable-stayed column can be reduced by increasing the flexural rigidity of the column or by increasing the moment resistance of the base plate assembly. The experimental anchor force data shown in figure 32 are entirely consistent with elementary theory. The largest tie-back forces occurred during test 1 (which employed fixed-base but relatively flexible W 4 x 13 columns) and tests 2 and 3 (which employed hinged-base columns). The smallest tie back forces occurred during tests 4, 5 and 6 (which used fixed-base and relatively stiff W 8 x 48 wide-flange columns).

Table 1. *Comparison of debris volume, flow velocity, and net deflection data*
[m^3, cubic meters; m/sec, meters per second; m, meters]

Characteristic	Test 1	Test 2	Test 3	Test 4	Test 5	Test 6
Debris volume (m^3)	9.8	9.6	10.3	10.4	10.4	10.1
Impact velocity of gravel spray (m/sec)	SM	12.5	NS	10.0	NS	10.0
Impact velocity of debris (m/sec)	SM	9.0	6.5	8.0	6.0	5.0
Outward deflection of net panel (m)	SM	1.46	0.30	1.93	0.40	1.50

SM = Data acquisition system malfunctioned
NS = No gravel spray due to presence of intervening sediment deposited during previous test

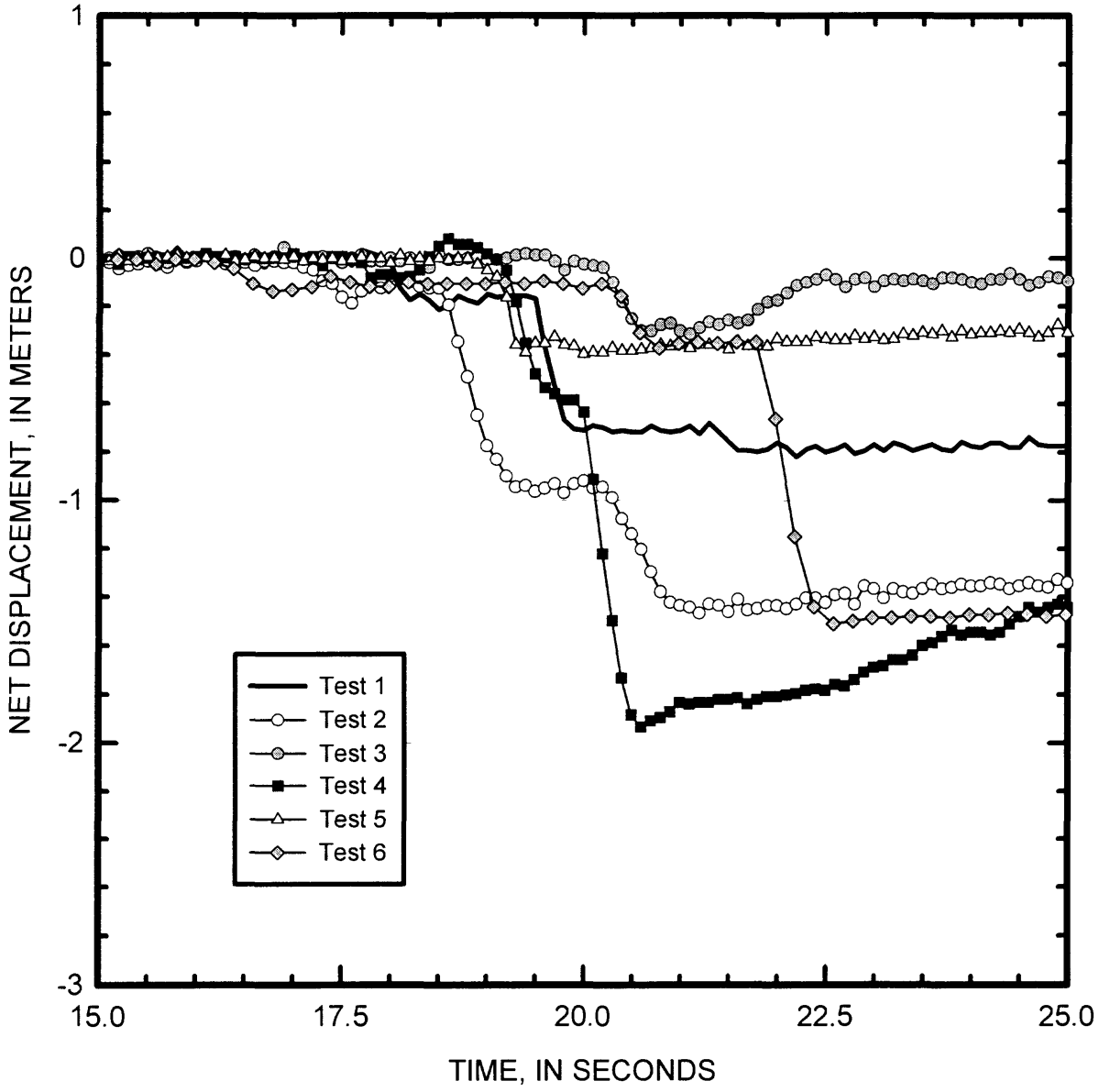

Figure 14. Net displacement data.

Table 2. *Comparison of barrier effectiveness in terms of debris containment*
[m^3, cubic meters]

Characteristic	Test 1	Test 2	Test 3	Test 4	Test 5	Test 6
Initial debris volume (m^3)	9.8	9.6	10.3	10.4	10.4	10.1
Volume passing through net (m^3)	SC	0.46	SC	0.12	.046	.0046
Percent passing (%)	SC	4.8	SC	1.2	0.44	0.05

SC = System collapsed

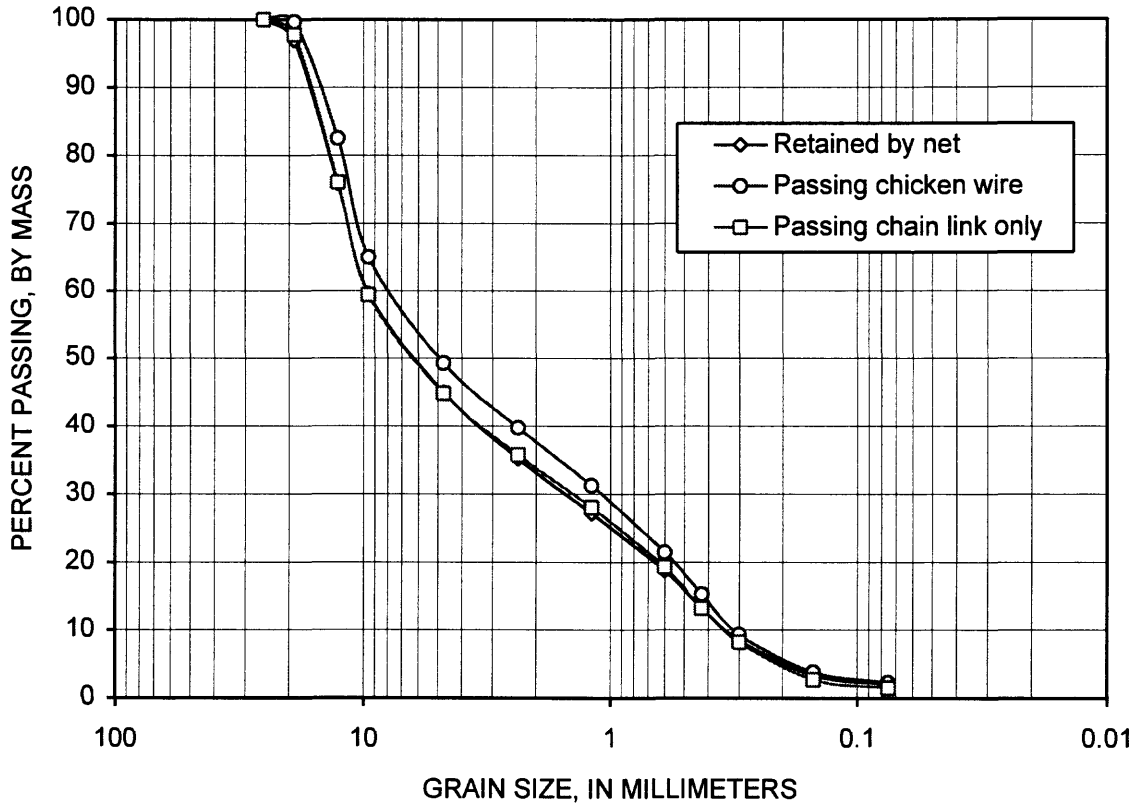

Figure 15. Comparison of gradations of retained and passing debris (test 2).

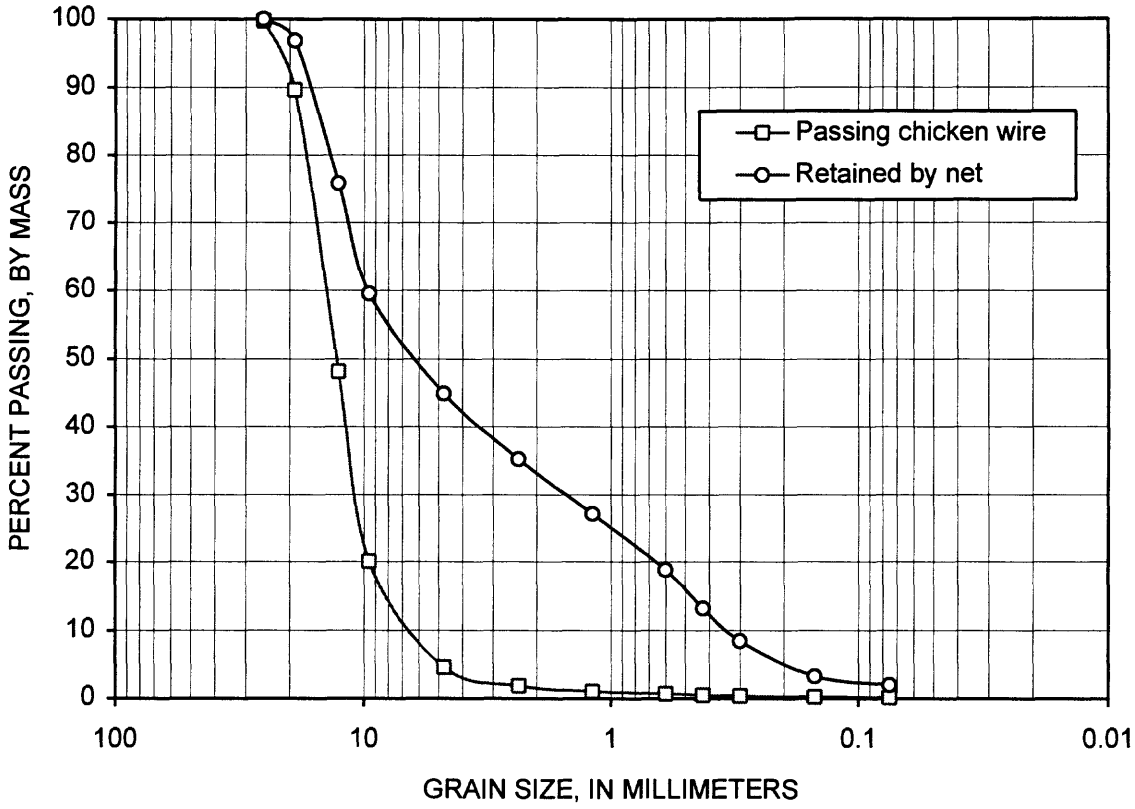

Figure 16. Comparison of gradations of retained and passing debris (test 4).

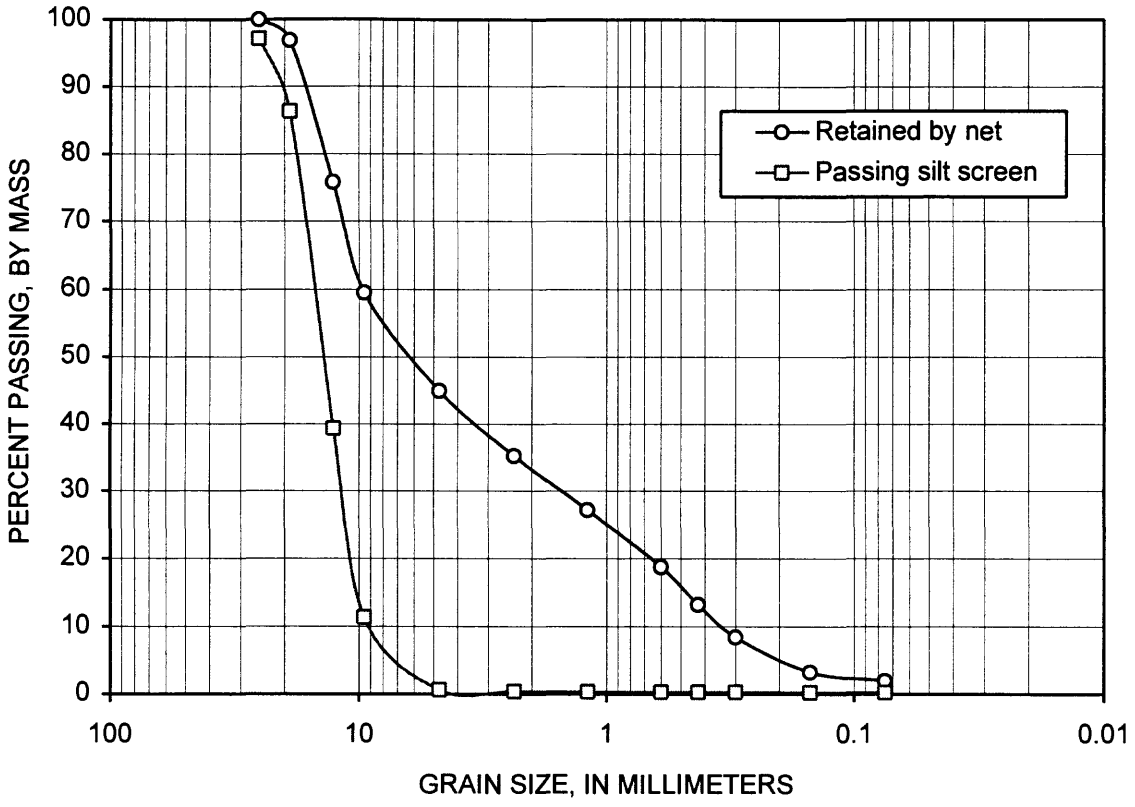

Figure 17. Comparison of gradations of retained and passing debris (test 6).

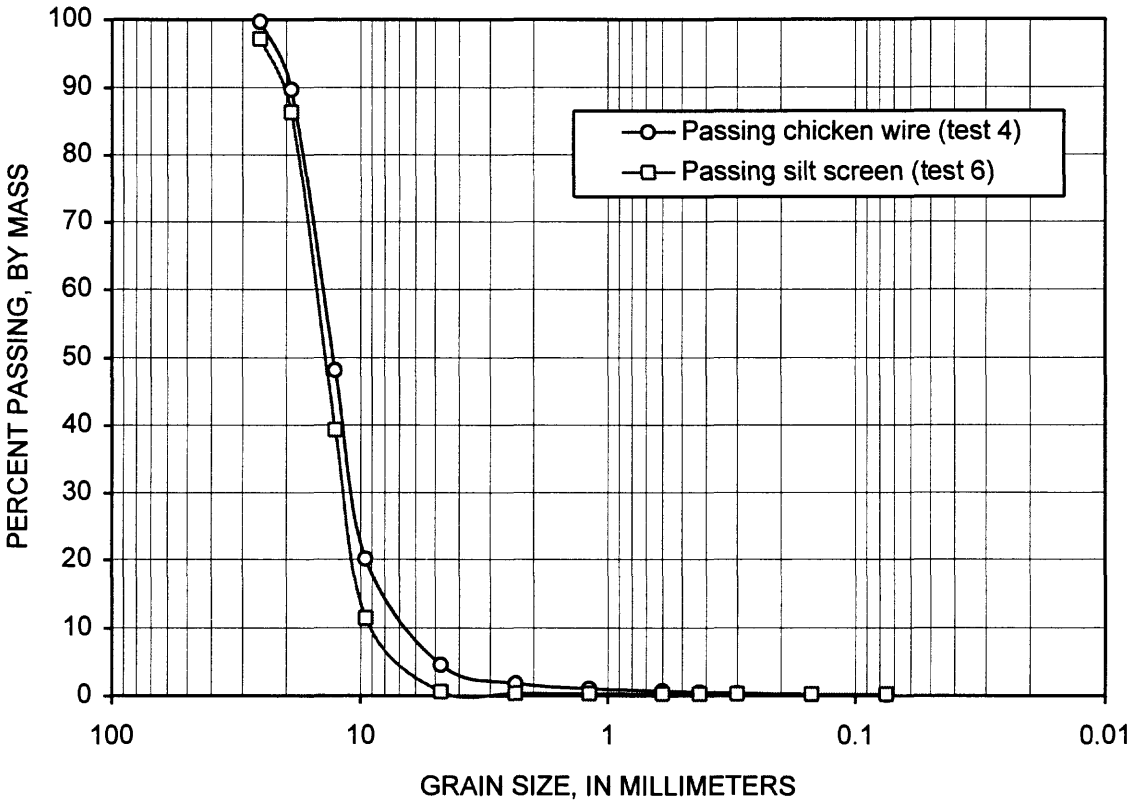

Figure 18. Comparison of debris passing the chicken wire (test 4) and silt screen (test 6) net liners.

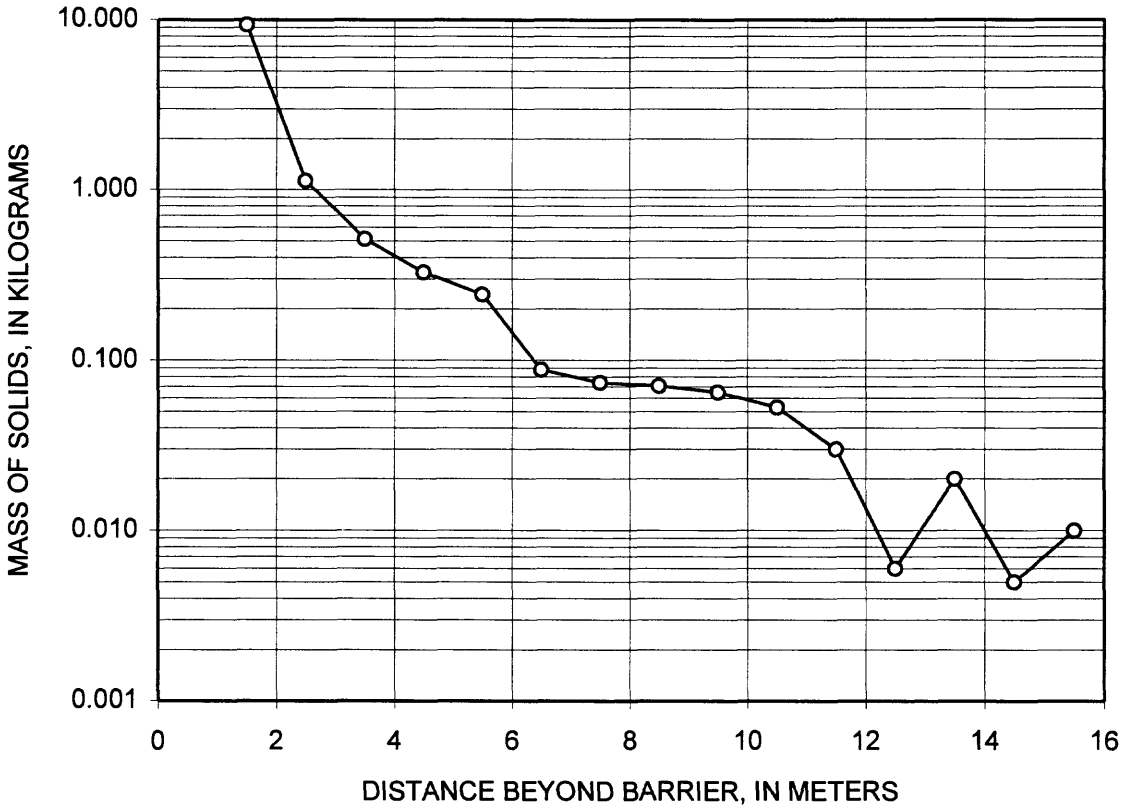

Figure 19. Distribution of debris passing beneath or through the barrier (test 6).

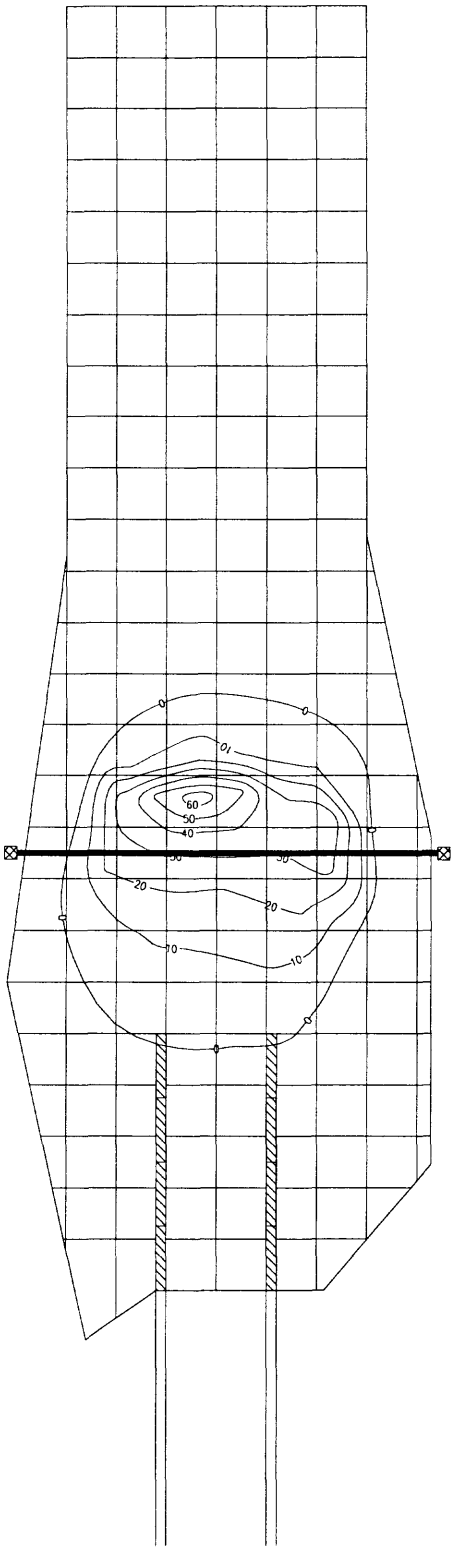

Figure 20. Contours of equal deposit thickness (in centimeters) for the debris flow of test 1.

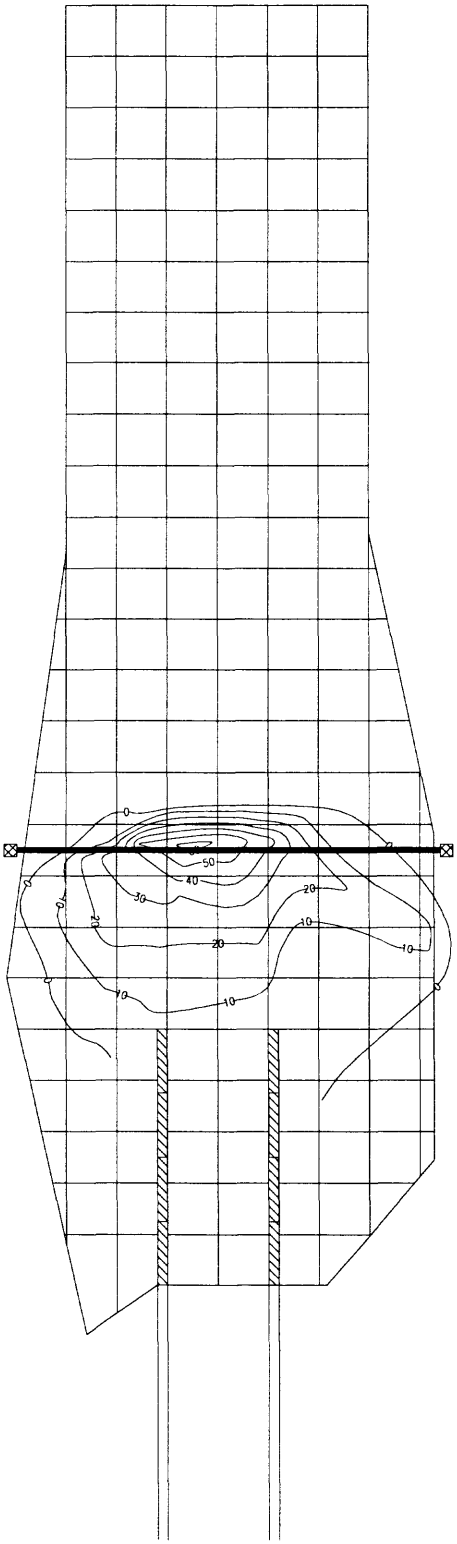

Figure 21. Contours of equal deposit thickness (in centimeters) for the debris flow of test 2.

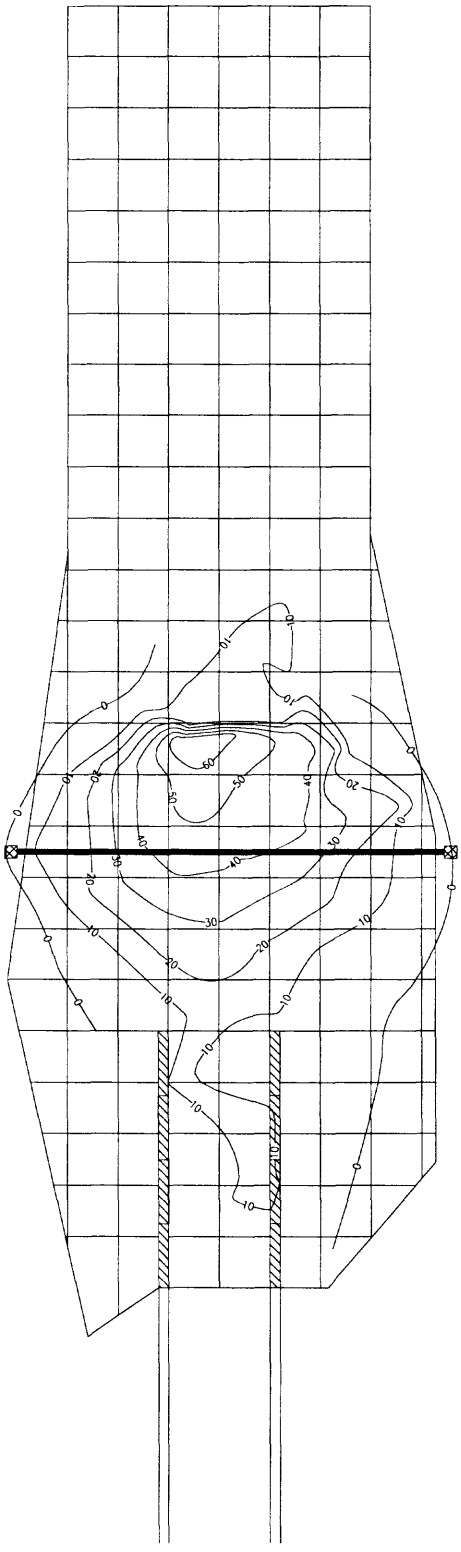

Figure 22. Contours of equal deposit thickness (in centimeters) for the debris flow of test 3.

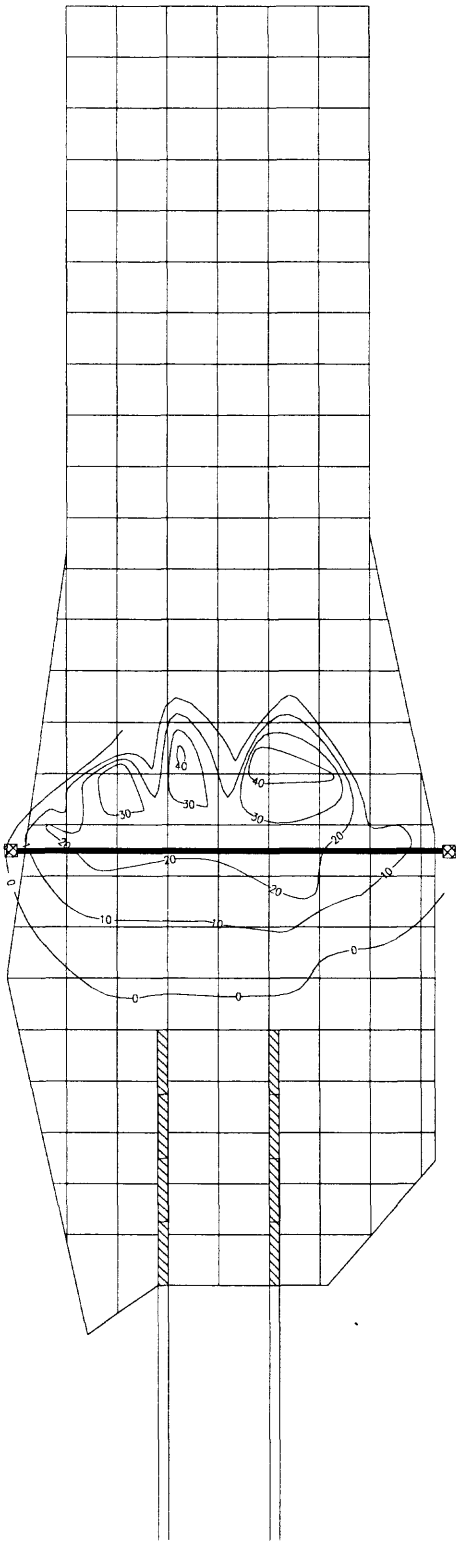

Figure 23. Contours of equal deposit thickness (in centimeters) for the debris flow of test 4.

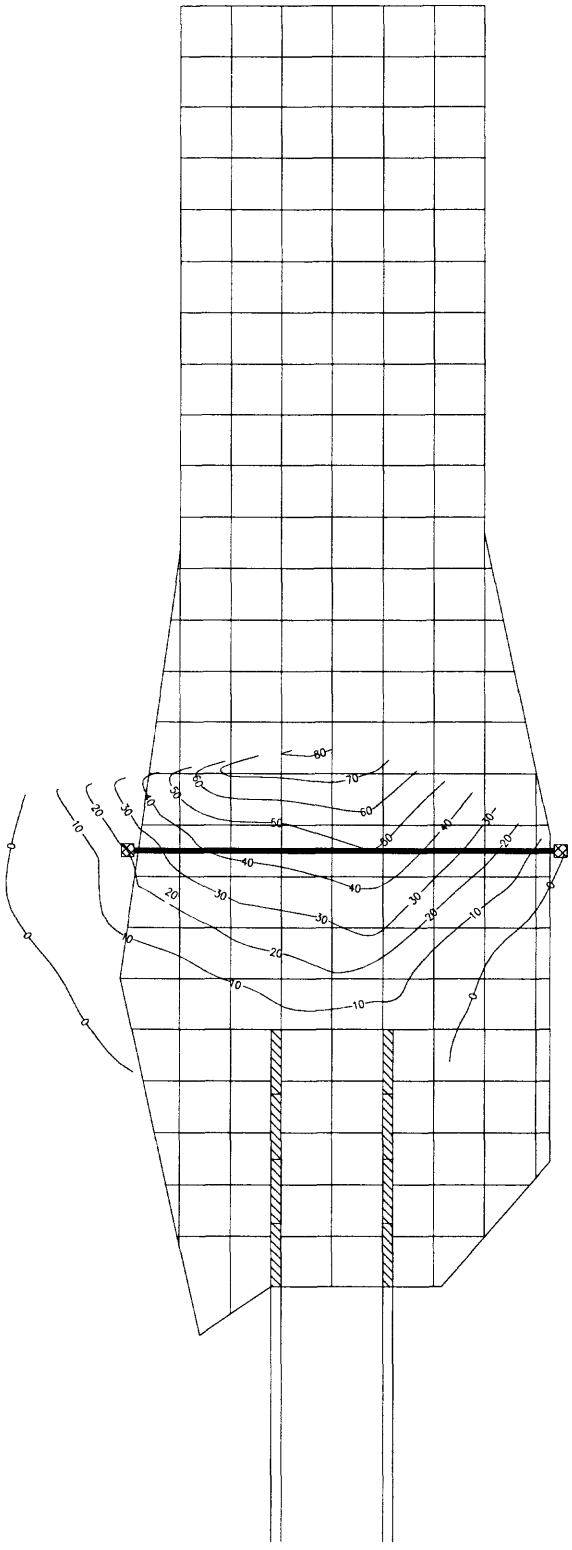

Figure 24. Contours of equal deposit thickness (in centimeters) for the debris flow of test 5.

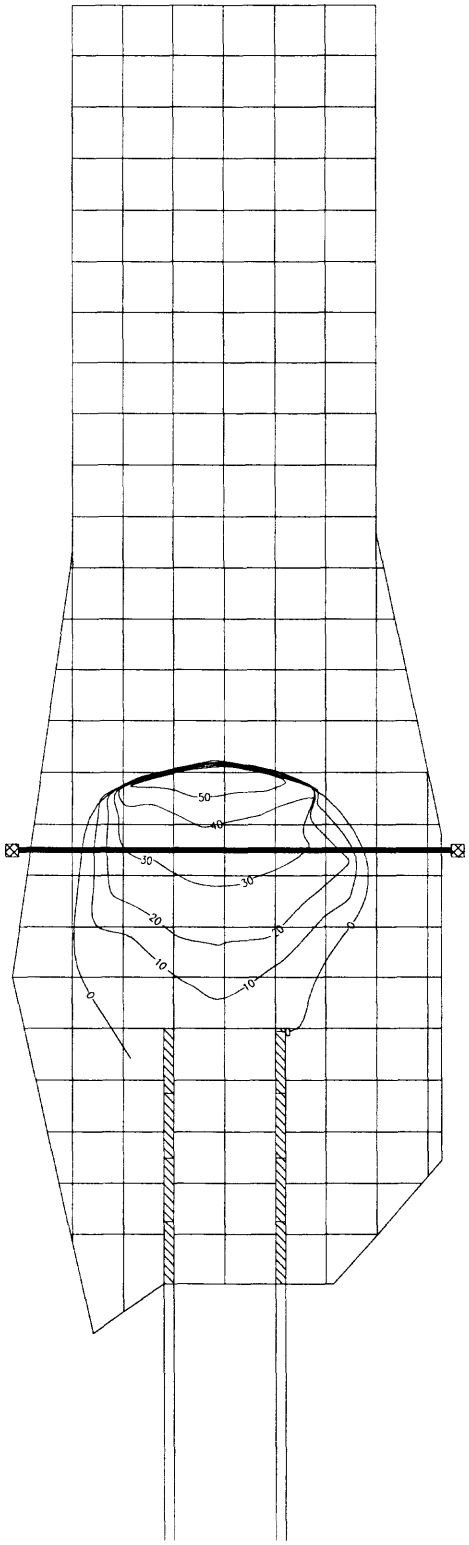

Figure 25. Contours of equal deposit thickness (in centimeters) for the debris flow of test 6.

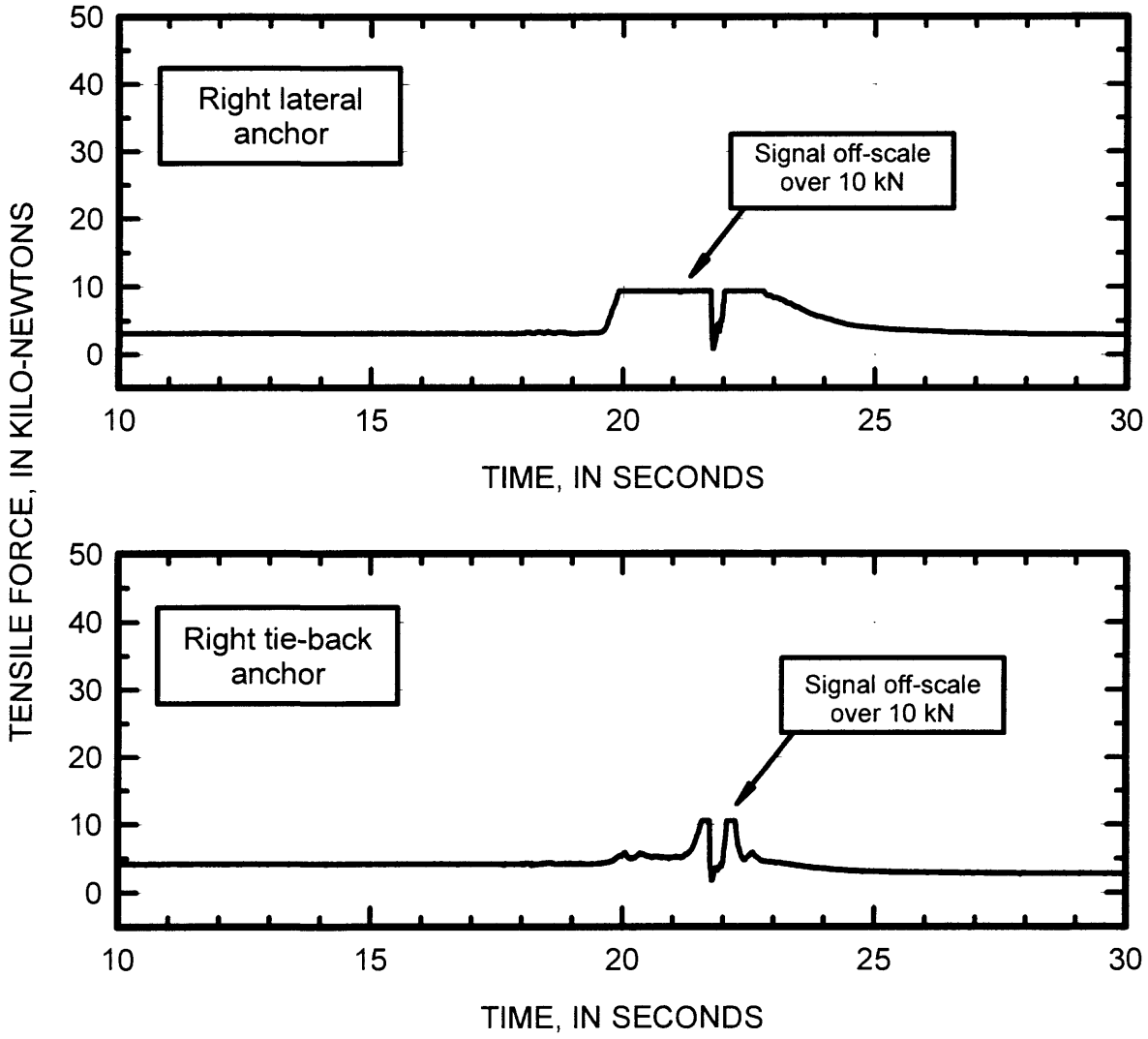

Figure 26. Anchor cable forces (Test #1).

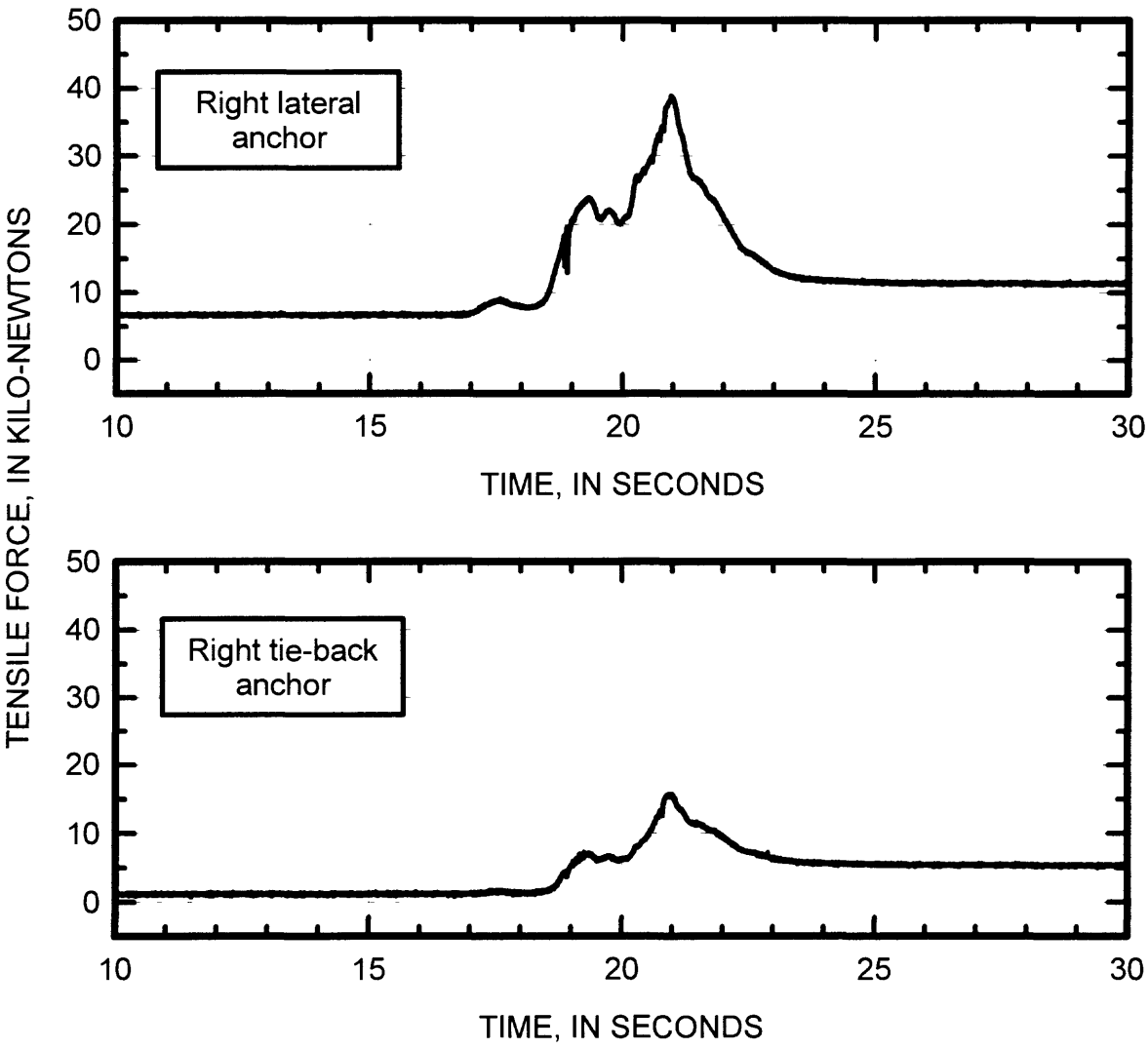

Figure 27. Anchor cable forces (Test #2).

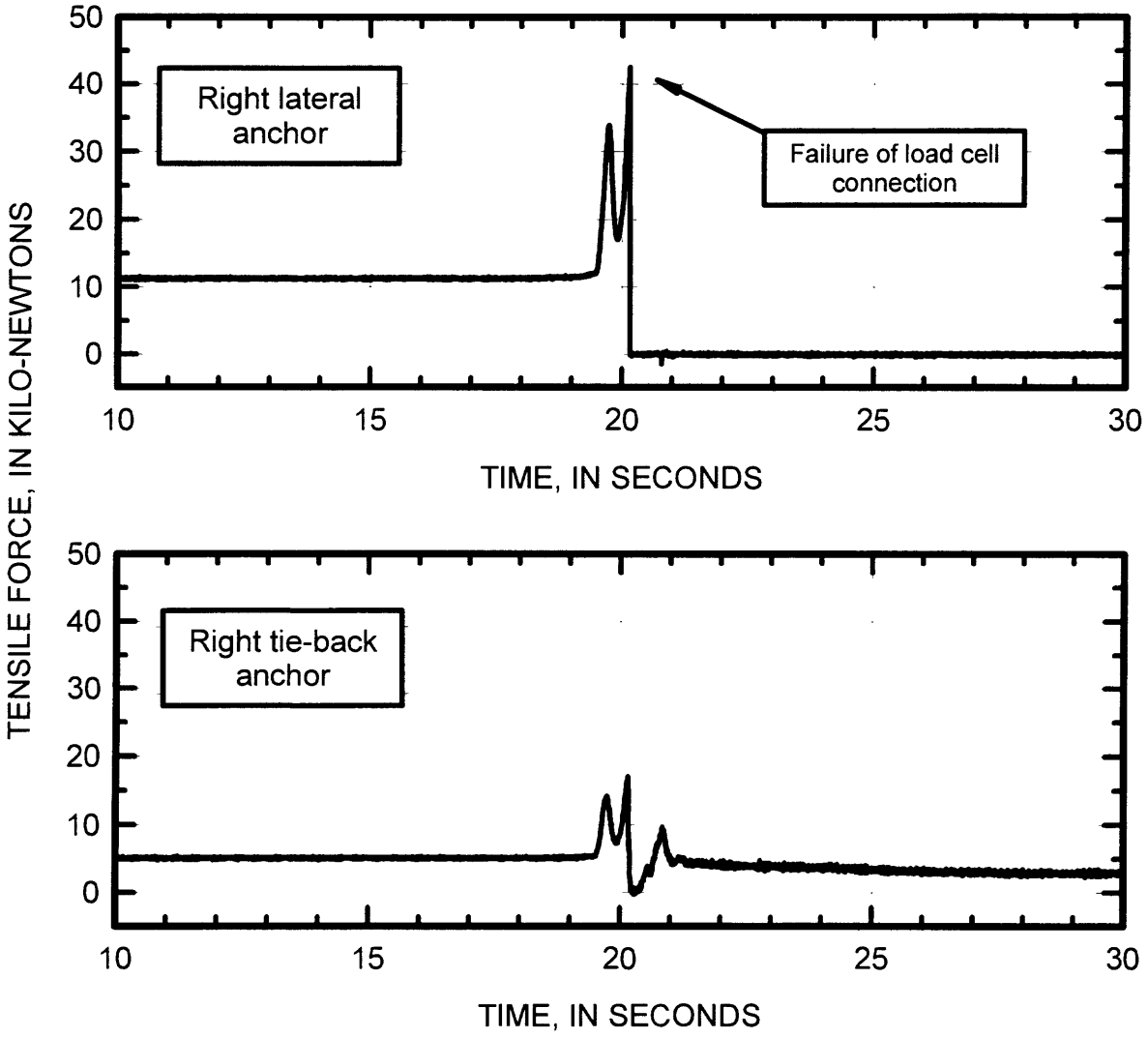

Figure 28. Anchor cable forces (Test #3).

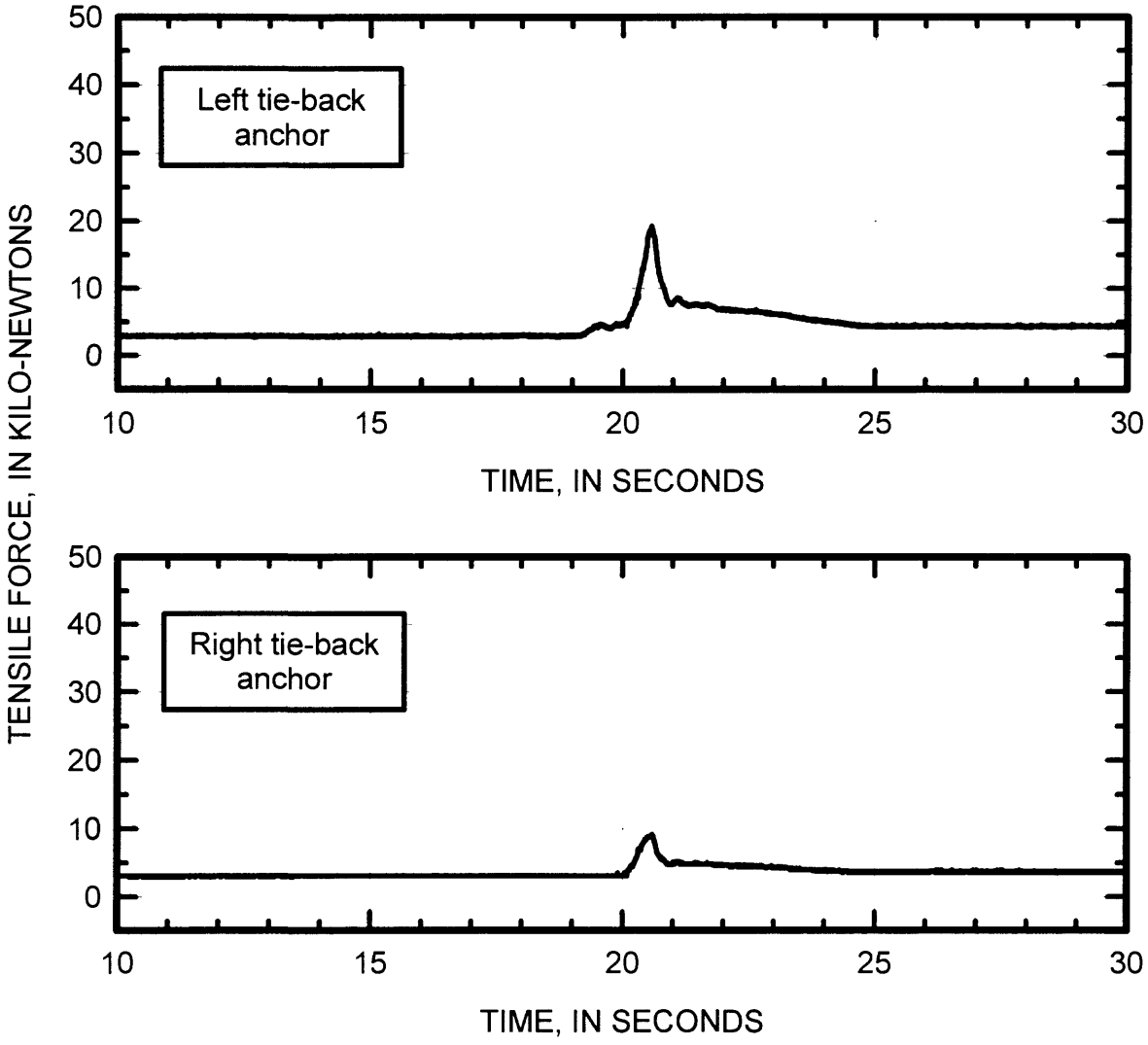

Figure 29. Anchor cable forces (Test #4).

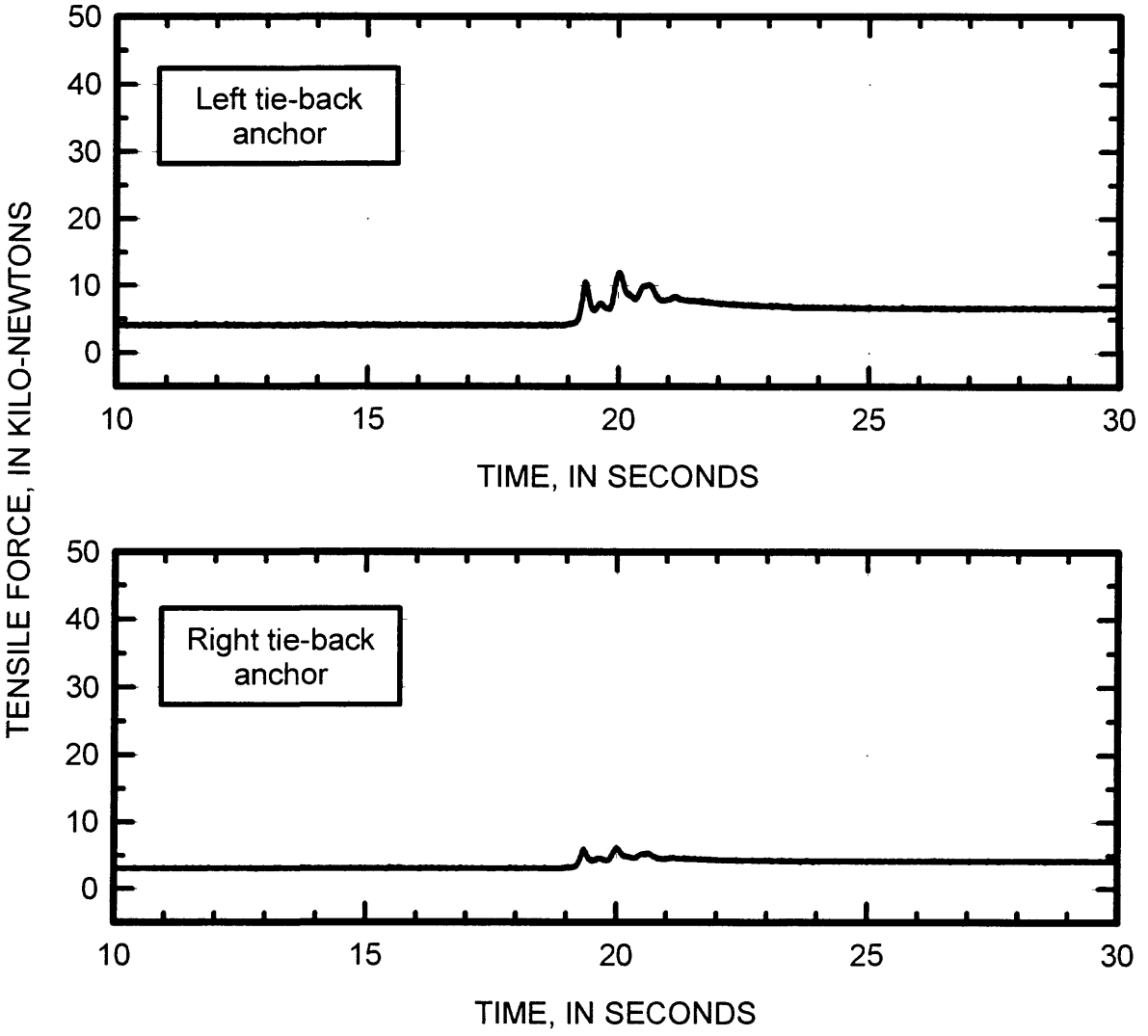

Figure 30. Anchor cable forces (Test #5).

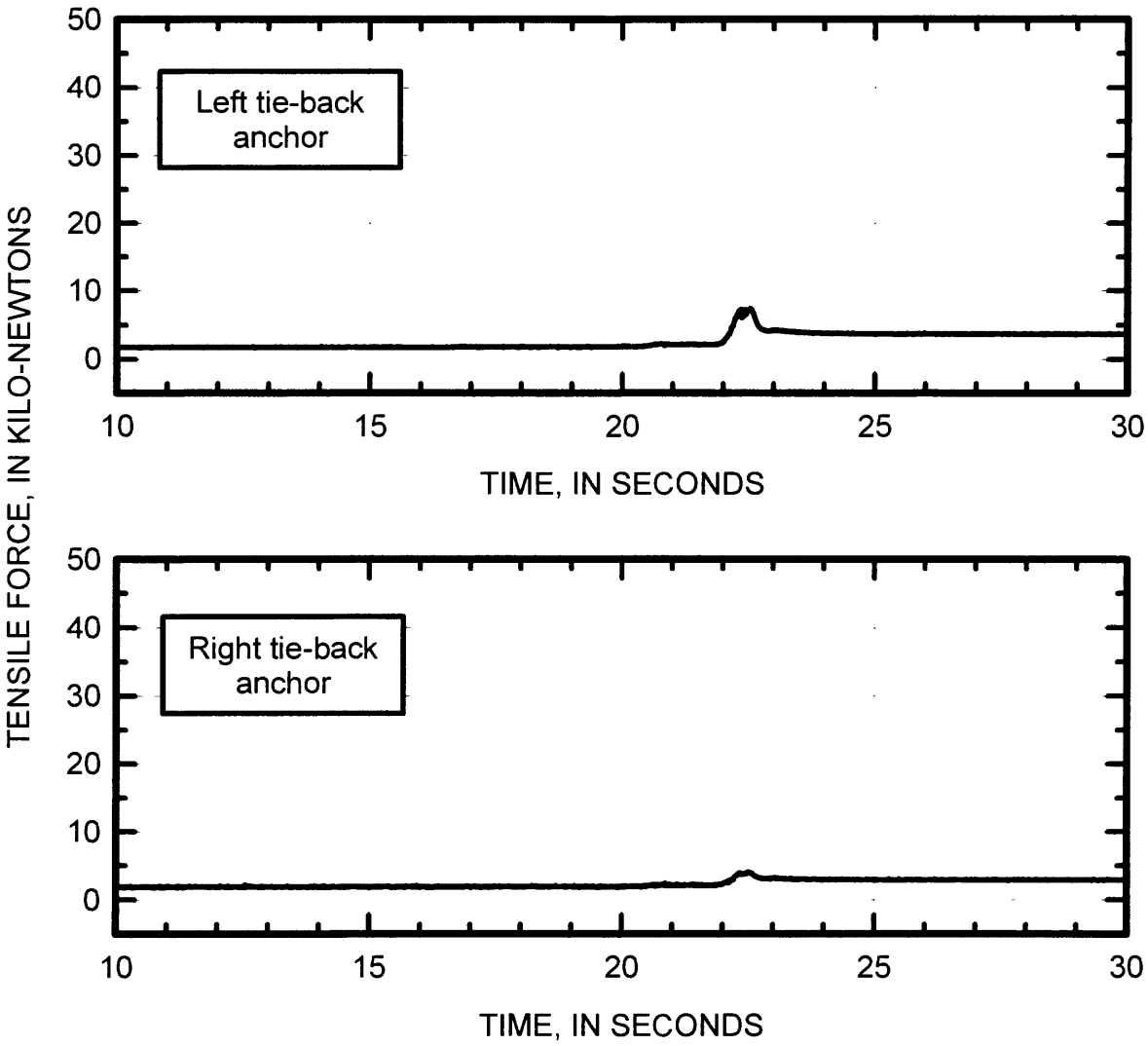

Figure 31. Anchor cable forces (Test #6).

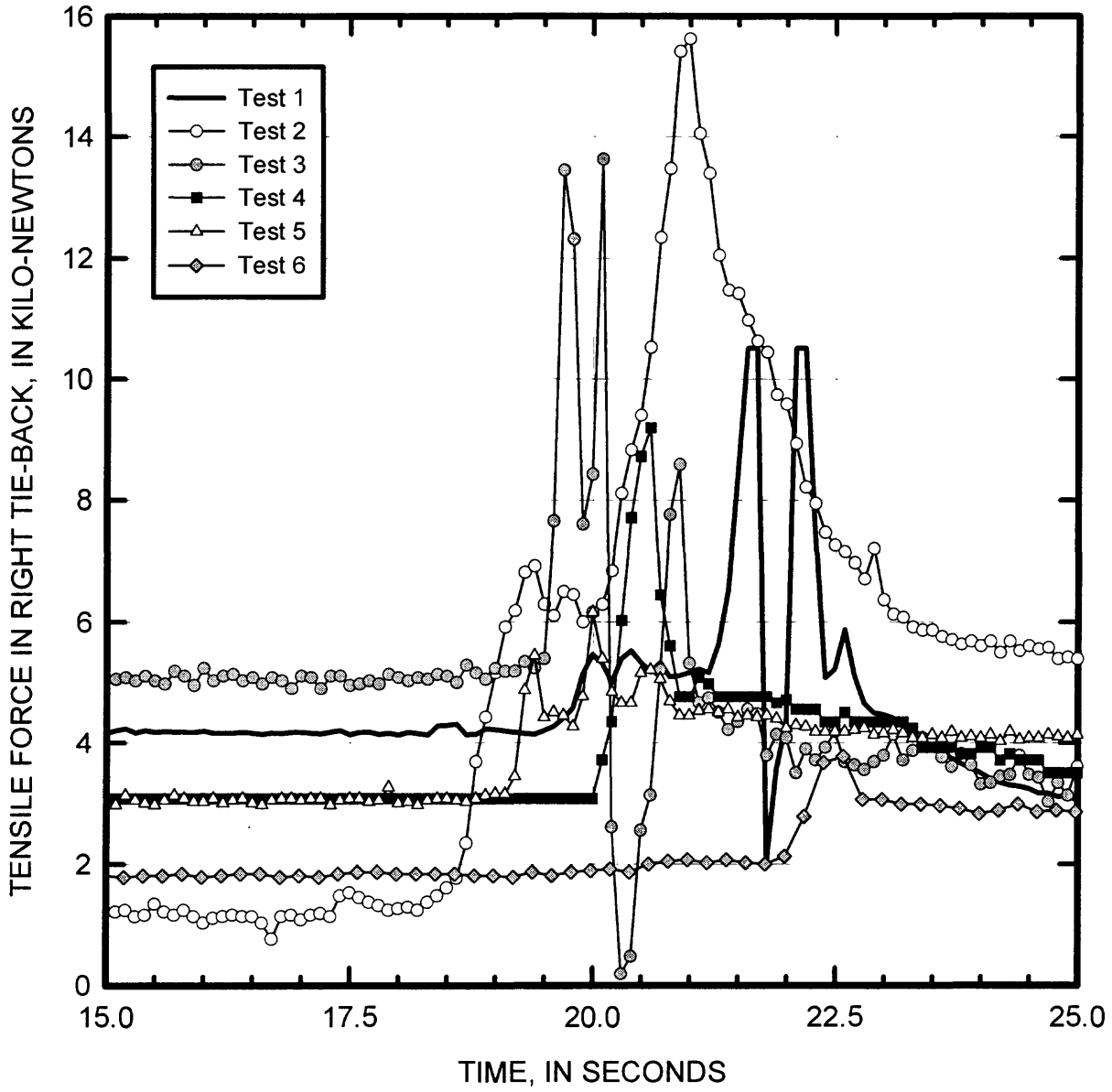

Figure 32. Comparison of right tie-back anchor cable forces.

SUMMARY

The experimental study described in this report permitted the evaluation of four flexible debris-flow mitigation systems. The moderate variety of options studied and the inherent variability of even a well-controlled, staged debris flow make it difficult to isolate the effect of any single parameter during a six-test study. Nevertheless, the testing program did provide much useful data. Both the 15 cm wire rope barrier and the 30 cm interlocking ring net barrier effectively stopped and contained the rapidly flowing sediment. Essentially full containment was realized in test 6, where less than 0.05 percent of the sediment passed beneath or through the net. These final two barrier systems may have the energy absorption and retention characteristics to effectively mitigate many small, natural debris flows.

REFERENCES

Duffy, J.D., and DeNatale, J.S., 1996, Debris flow mitigation using flexible barriers, Proceedings of the 47th Annual Highway Geology Symposium, p. 243-252.

Iverson, R.M., 1997, The physics of debris flows, Reviews of Geophysics, v. 35, no. 3, p. 245-296.

Iverson, R.M., LaHusen, R.G., and Costa, J.E., 1992, Debris-flow flume at H.J. Andrews Experimental Forest, Oregon, U.S. Geological Survey Open-File Report 92-483, 2 p.

Major, J.J., Iverson, R.M., McTigue, D.F., Macias, S., and Fiedorowicz, B.K., 1997, Geotechnical properties of debris-flow sediments and slurries, Proceedings of the First International Conference on Debris-Flow Hazards Mitigation, p. 249-259.